Shock-wave structure in a partially ionized gas

By M. S. GREWAL† AND L. TALBOT
Division of Aeronautical Sciences, University of California, Berkeley

(Received 8 January 1963)

The structure of a shock wave in a partially ionized gas, which may be in thermal non-equilibrium ahead of the shock wave, is investigated. A method is developed to solve this problem by separating it into two parts. First, the structure of the shock wave associated with the massive particles, ions and atoms, is assumed to be of the Mott-Smith form. Then the behaviour of the electrons as they pass though this shock is analysed. Using this method, calculations are carried out for shock waves at several Mach numbers and several values of the electron-ion temperature ratio ahead of the shock. An essential feature of the shock profiles is found to be the existence of a broad zone of elevated electron temperature ahead of the electron compression region, caused by the high thermal conductivity in the electron gas.

1. Introduction

The complete analysis of the structure of a steady plane shock wave in a partially ionized gas consists of determining the density, velocity, and temperature profiles of each of the species. At least three species must be considered: ions, atoms and electrons. The basic equations are the mass, momentum, and energy-transport relations for each species, such as, for example, the Navier–Stokes equations and associated diffusion relations which follow from kinetic theory using the Navier–Stokes approximation, together with the appropriate Maxwell equations.

The mathematical complication of such an analysis makes it necessary to seek certain simplifying approximations. The approximations we shall make use of are based on the following physical properties of a slightly ionized gas:

(i) The energy content of the electrons is only a small fraction of the total internal energy of the gas.

(ii) Because the electron mass is much smaller than the ion-atom mass (only singly ionized monatomic gases will be considered), the rate of energy exchange between electrons and massive particles is slow. Also, because of their almost equal mass, the ions and the neutral atoms have essentially the same mass-motion velocity, in the absence of external fields, and are the primary contributors to the viscous stress (momentum exchange) in the gas.

(iii) On the other hand, the electrons, because of their high mobility, are effective in transporting thermal energy within the electron gas, although this energy is only very slowly communicated to the massive particles.

† Now at Aerospace Corporation, El Segundo, California.

(iv) Finally, for all but very feebly ionized gases, the deviations from charge neutrality are negligible in comparison to the charge concentrations. Charge neutrality implies that in the absence of electric current the electrons and massive particles have the same mass-motion velocity.

These properties lead us to adopt the following model for a shock wave in a partially ionized gas. The massive particles undergo a shock which is essentially uninfluenced by the presence of the electrons, and which is governed only by the transport properties and Mach number of the ion-atom mixture. The electrons, which are 'subsonic' with respect to the ion-atom Mach number, are compressed in passing through the ion-atom shock, and follow the density variation of the massive particles. However, because of the high electron thermal conductivity, the electron temperature within the shock zone may deviate appreciably from the ion-atom temperature, and the electrons will only very slowly come to equilibrium with the massive particles through relaxation. According to this model, the ion-atom shock acts as a kind of 'forcing function' on the electrons, and if the ion-atom shock structure is known beforehand, the only unknown in the problem is the electron temperature profile. It is important to note that the energy required to compress and heat the electrons comes from the ion-atom mixture (through energy exchange and a slight departure from charge neutrality, as will be discussed later on) and not from the kinetic energy of the electrons, which is negligible.

The form of the ion-atom shock structure which we shall use is the Mott-Smith (1951) solution. There is some reason to suppose (cf. Talbot 1962) that the Mott-Smith solution may be more accurate than the Navier–Stokes solution for high Mach numbers. For our purposes, moreover, the Mott-Smith solution is more convenient than the Navier–Stokes solution, since it provides us with a simple analytical representation of the massive-particle shock profile. In parts of the analysis the Mott-Smith profiles are replaced by delta and Heaviside functions.

We are not aware of any published work on the detailed structure of a shock wave in a partially ionized gas. Several studies have been made of shock waves in fully ionized gases, especially the proton-electron gas. In particular, Jukes (1957) analysed this shock-structure problem by means of the Navier–Stokes equations, neglecting the thermal conductivity of the protons and the viscosity of the electrons. His results predict a broad zone of elevated electron temperature ahead of the massive-particle shock, as is predicted by the present analysis. Tidman (1958) attacked the same problem by using the Fokker–Planck equation, in the spirit of Mott-Smith. He, however, in effect assumed zero thermal conductivity for the electron gas. According to Tidman's analysis, the ions are heated by an initial shock, and the electrons at the end of this shock are still at their upstream temperature. The shock is followed by a relaxation zone, in which the electrons and ions equilibrate. However, according to Jukes's results and (as will be seen) the present analysis, the electrons are very nearly at their final equilibrium temperature at the end of the ion shock. Thus it appears that the neglect of the electron thermal conductivity results in the loss of an essential feature of the shock structure in an ionized gas.

Another study of some interest is the work of Greenberg, Sen & Treve (1960). Here the shock structure problem in a fully ionized gas was treated with the neglect of the viscosity and thermal conductivity of both the electrons and protons, as well as the neglect of momentum and energy transfer between these species. Charge neutrality was not assumed, however, and diffusion was taken to be the shock-broadening mechanism. Greenberg *et al.* predict an oscillatory structure for both the electric field and the electron velocity, but their results are restricted to Mach numbers less than two, above which they were unable to find a continuous solution between the upstream and downstream boundary conditions. According to these authors, the oscillatory electric field constitutes a 'fine structure' to the non-oscillating field obtained by Jukes, but because of the nature of their assumptions, it is difficult to know how much physical significance may be attached to their results.

2. Electron energy equation

The flow of the gas is taken to be along the x-axis from $-\infty$ to $+\infty$; $x = 0$ is taken as the centre of the ion-atom shock. For one-dimensional steady flow in the absence of applied electric and magnetic fields, the electron energy equation (see Kaufman 1960, for example) can be written as

$$\tfrac{3}{2}u\frac{d}{dx}(n_e kT_e) = -\tfrac{5}{2}n_e kT_e\frac{du}{dx} - \frac{dQ}{dx} + \Phi - R^{em} - uP^{em}, \tag{2.1}$$

in which u is the electron mean velocity, n_e and T_e the electron number density and temperature, and k Boltzmann's constant. The heat flux Q is given by $-k\lambda_e(dT_e/dx)$, where $k\lambda_e$ is the electron thermal conductivity, and P^{em} and R^{em} denote the momentum and energy transfer rates from the electrons to the massive particles per unit volume, respectively. When the electrons and massive particles have the same mean velocity, P^{em} vanishes. As usual, Φ represents the viscous dissipation, given by $\frac{4}{3}\mu_e(du/dx)^2$, where μ_e is the electron gas viscosity. The degree of ionization is assumed constant, and energy transfers due to ionization-recombination processes are neglected in (2.1). A discussion of this point will be given later.

For the transport properties of the electron gas we shall take the values appropriate to a fully ionized gas, so that $\mu_e \sim T_e^{\frac{5}{2}}$ and $\lambda_e \sim T_e^{\frac{5}{2}}$. Moreover, we shall assume that the energy transfer term is that given by Post (1956)

$$R^{em} = \left(\frac{32\pi}{km_e}\right)^{\frac{1}{2}}\frac{m_e n_e^2}{m_i T_e^{\frac{3}{2}}}e^4 \ln\Lambda\ (T_e - T_i), \tag{2.2}$$

in which the as yet undefined quantities are the ion temperature T_i, the ion and electron masses m_i and m_e, the absolute value of the electronic charge e, and the Coulomb logarithm Λ (Spitzer 1956). The use of (2.2) for R^{em} implies that the ionization, though slight, is sufficiently large that ion-electron collisions dominate over electron-neutral collisions, because of the large Coulomb cross-section. However, the use of (2.2) is not essential, since it merely provides a convenient representation for the energy transfer term, and if the conditions implied in its use were far from being realized a more appropriate energy transfer term could

be used in its stead without changing any essential features of the analysis. The same comments apply to μ_e and λ_e.

We non-dimensionalize (2.1) by referring all quantities to their upstream values, so that $T_e/T_{e_0} = \theta$, $T_i/T_{e_0} = \phi$, $n_e/n_{e_0} = \nu$, $\lambda_e/\lambda_{e_0} = \mu_e/\mu_{e_0} = \theta^{\frac{1}{2}}$, and we introduce the non-dimensional distance $\xi = x/L$, where L is a characteristic length, taken to be the ion-atom shock thickness. We obtain, using the assumption that $n_i = n_e$, $u_i = u_e$ everywhere,

$$\frac{d}{d\xi}\left(\theta^{\frac{5}{2}}\frac{d\theta}{d\xi}\right) - a\frac{d\theta}{d\xi} + \tfrac{2}{3}a\left(\frac{1}{\nu}\frac{d\nu}{d\xi}\right)\theta + \frac{b}{\nu^4}\left(\frac{d\nu}{d\xi}\right)^2\theta^{\frac{5}{2}} - \frac{c\nu^2}{\theta^{\frac{3}{2}}}(\theta-\phi) = 0, \tag{2.3}$$

in which the constants a, b, c are given by

$$a = \tfrac{3}{2}L\frac{n_{e_0}u_0}{\lambda_{e_0}}, \quad b = \frac{4}{3}\frac{\mu_{e_0}u_0^2}{(kT_{e_0})\lambda_{e_0}}, \quad c = \frac{n_{e_0}^2L^2}{(kT_{e_0})^{\frac{3}{2}}\lambda_{e_0}}\frac{(32\pi m_e)^{\frac{1}{2}}}{m_i}e^4\ln\Lambda. \tag{2.4}$$

Convenient expressions for a, b, c are given in the Appendix. From the relative magnitudes of a and b it can be shown that the electron viscous dissipation term is very small, the ratio b/a being of the order of 5×10^{-3} for a typical case. Henceforth the dissipation term will be neglected.

For the ion-atom shock quantities ν and ϕ, we taken the Mott-Smith results, which are

$$\nu = 1 + \frac{3\beta_1}{1+e^{-4\xi}}, \tag{2.5a}$$

$$\phi = \frac{(M^2+3)}{M^2+3+4M^2e^{4\xi}} + \beta_2\frac{M^2e^{4\xi}}{(M^2+3)+4M^2e^{4\xi}} + \beta_3\frac{M^2(M^2+3)e^{4\xi}}{[M^2+3+4M^2e^{4\xi}]^2}. \tag{2.5b}$$

The constants β_1, β_2, β_3 are functions of the free-stream Mach number M based on the sound speed in the ion-atom mixture,

$$\beta_1 = \frac{M^2-1}{M^2+3}, \quad \beta_2 = \frac{(M^2+3)(5M^2-1)}{4M^2}, \quad \beta_3 = \frac{5(M^2-1)^2}{4M^2}. \tag{2.6}$$

For high Mach numbers we may take $\beta_1 = 1$, which then gives

$$\nu = 1 + \frac{3}{1+e^{-4\xi}}, \quad \frac{1}{\nu}\frac{d\nu}{d\xi} \equiv f(\xi) = \frac{12e^{-4\xi}}{(1+e^{-4\xi})(4+e^{-4\xi})}. \tag{2.7a}$$

Also for large M,

$$\phi = \frac{1}{1+4e^{4\xi}}\left\{1+\beta_2e^{4\xi}+\frac{\beta_3e^{4\xi}}{1+4e^{4\xi}}\right\}. \tag{2.7b}$$

The quantities ν and f, which are central to the analysis, are plotted in figure 1.

Upon making the aforementioned simplifications and substitutions, the governing equation for the electron temperature can be written

$$\frac{2}{7}\frac{d^2\theta^{\frac{7}{2}}}{d\xi^2} = a\frac{d\theta}{d\xi} - \tfrac{2}{3}a\theta f(\xi) + \frac{c\nu^2}{\theta^{\frac{3}{2}}}(\theta-\phi), \tag{2.8}$$

with $f(\xi)$ and $\nu(\xi)$ given by (2.7a) and $\phi(\xi)$ given by (2.7b). The boundary conditions associated with (2.8) are

$$\phi(-\infty) = \theta(-\infty) \equiv \theta_0 = 1, \quad \theta(+\infty) \equiv \theta_1 = \phi_1 \tag{2.9a}$$

and

$$(d\theta/d\xi)_{\xi=\pm\infty} = 0, \tag{2.9b}$$

where ϕ_1 is the value of ϕ at $\xi = +\infty$ as given by (2.5). These boundary conditions are for the case when the electrons ahead of the shock are in thermal equilibrium with the ion-atom mixture. The boundary conditions for the non-equilibrium case will be discussed subsequently.

Equation (2.8) is a non-linear equation, with singularities at both end-points. To bring out the essential features of the shock transition, we shall present solutions to (2.8) under several different simplifying assumptions. First, we

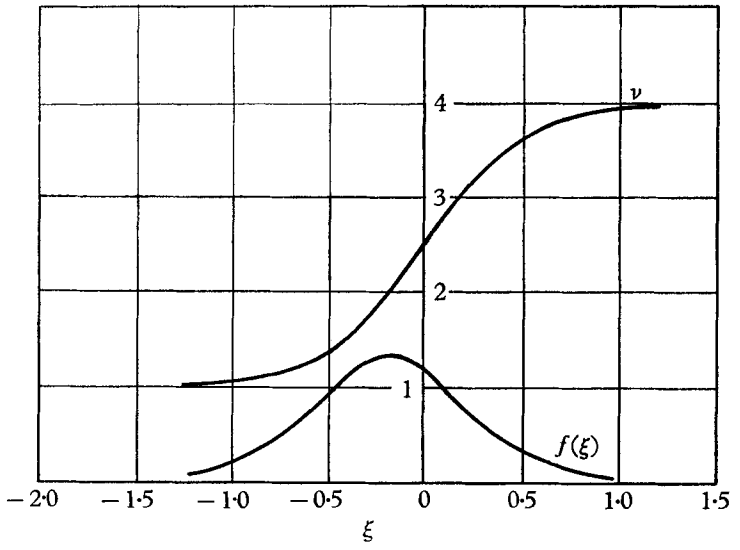

FIGURE 1. Non-dimensional density and density gradient for a normal shock wave according to Mott-Smith theory *vs* the non-dimensional distance $\xi = x/L$, where L is the thickness of the massive-particle shock wave. Functions plotted are those given in (2.7*a*).

$$\nu = \frac{4+e^{-4\xi}}{1+e^{4\xi}} = \frac{1+4e^{4\xi}}{1+e^{4\xi}},$$

$$f(\xi) = \frac{1}{\nu}\frac{d\nu}{d\xi} = \frac{12e^{-4\xi}}{(4+e^{-4\xi})(1+e^{-4\xi})}.$$

consider the case of constant thermal conductivity and neglect relaxation effects. Following this we treat the case of temperature-dependent thermal conductivity with relaxation. And finally, we consider the latter case when the electrons and ion-atom mixture are not in thermal equilibrium ahead of the shock.

3. Constant thermal conductivity, no relaxation

When the thermal conductivity is taken constant, and relaxation effects are neglected, (2.8) reduces to

$$\frac{d^2\theta}{d\xi^2} = a\frac{d\theta}{d\xi} - \tfrac{2}{3}af(\xi)\,\theta. \tag{3.1}$$

The boundary conditions at $\xi = -\infty$ are $\theta_0 = 1$, $(d\theta/d\xi)_0 = 0$. At $\xi = +\infty$ we require $(d\theta/d\xi) = 0$, but because relaxation has been omitted, we cannot in advance

specify θ_1, but must determine it in the course of the solution. The problem thus posed is not physically realistic, since it assumes that the electrons and heavy particles are completely insulated from one another, which would be possible only if $m_e/m_i \equiv 0$. However, there are a number of interesting features to this problem which provide insight for the more realistic cases to be treated subsequently.

An asymptotic solution to (3.1) for $\xi \to -\infty$ is obtained by transforming (3.1) to an integral equation. We first integrate (3.1) from $-\infty$ to ξ,

$$\frac{d(\theta-1)}{d\xi} - a(\theta-1) = -\tfrac{2}{3}a \int_{-\infty}^{\xi} f(t)\,\theta(t)\,dt. \tag{3.2}$$

Then after multiplying by the integrating factor $e^{-a\xi}$ and integrating once again, we obtain

$$e^{-a\xi}(\theta-1) - K = -\tfrac{2}{3}a \int_{-\infty}^{\xi} e^{-as}\,ds \int_{-\infty}^{s} f(t)\,\theta(t)\,dt, \tag{3.3}$$

where we have written $K = \lim_{\xi \to -\infty} e^{-a\xi}(\theta-1)$. It can be shown that this limit exists and is finite. Then using the asymptotic form $f(\xi) \sim 12e^{4\xi}$, and interchanging the order of integration, we obtain

$$\theta = 1 + K\,e^{a\xi} + 8\int_{-\infty}^{\xi} e^{4s}\,\theta(s)\,ds - 8e^{a\xi}\int_{-\infty}^{\xi} e^{(4-a)s}\,\theta(s)\,ds. \tag{3.4}$$

This integral equation may be solved by the method of successive approximations (cf. Tricomi 1957). The first two approximations are

$$\theta^{(0)} = 1 + K\,e^{a\xi}, \quad \theta^{(1)} = 1 + K\,e^{a\xi} - \frac{2a}{(4-a)}e^{4\xi} - \frac{2aK}{(4+a)}e^{(4+a)\xi}. \tag{3.5}$$

The method fails for a equal to multiples of 4, but we shall be interested only in $a < 4$.

In similar fashion, an asymptotic expansion for $\xi \to +\infty$ may be obtained, which has the form, to second approximation

$$\theta^{(0)} = \theta_1, \quad \theta^{(1)} = \theta_1\left[1 - \frac{a}{2a+8}\,e^{-4\xi}\right]. \tag{3.6}$$

Each of the asymptotic expansions contains one unknown parameter, to be determined from the boundary conditions at the other end. One way to complete the solution is to continue the asymptotic solutions from both ends by numerical integration and by repeated trial find the pair of values K and θ_1 which correspond to a continuous integral curve joining the two asymptotic solutions. We shall employ a simpler though less accurate method.

We take $\theta(\xi)$ for the entire domain $(-\infty \leqslant \xi \leqslant +\infty)$ as

$$\left.\begin{aligned} \theta(\xi) &= 1 + K\,e^{a\xi} && (\xi \leqslant -1{\cdot}0), \\ \theta(\xi) &= \theta_1(1 - \tfrac{1}{2}a(4+a)^{-1}e^{-4\xi}) && (\xi \geqslant 0{\cdot}5), \\ \theta(\xi) &= \alpha_0 + \alpha_1\xi + \alpha_2\xi^2 + \alpha_3\xi^3 && (-1{\cdot}0 \leqslant \xi \leqslant 0{\cdot}5). \end{aligned}\right\} \tag{3.7}$$

The values $\xi = -1{\cdot}0, +0{\cdot}5$ at which the polynomial is matched to the asymptotic expansions were arbitrarily chosen to correspond to locations where the forcing function $f(\xi)$ (see figure 1) is less than about one-fourth of its maximum value. The four coefficients α_n of the polynomial are expressed in terms of K and θ_1 by requiring that the polynomial and its first derivative match the asymptotic

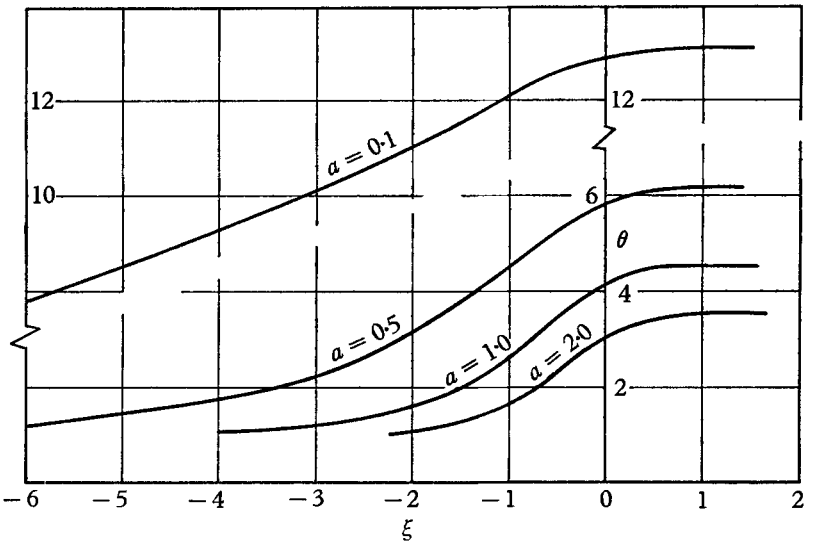

FIGURE 2. Variation of electron temperature θ through shock wave for different values of the parameter a, under assumptions of constant thermal conductivity and no relaxation effects.

expansions at both $\xi = -1{\cdot}0$ and $\xi = 0{\cdot}5$. Then the evaluation of K and θ_1 proceeds as follows. From (3.2) and (2.9*b*) we have

$$\theta_1 = 1 + \frac{2}{3}\int_{-\infty}^{\infty} f(t)\,\theta(t)\,dt. \tag{3.8}$$

On the other hand, (3.2) may be integrated and rearranged to read

$$\theta_1 = 1 + a \lim_{\xi\to\infty} \int_{-\infty}^{\xi} (\theta - 1)\,dt - \frac{2}{3}\int_{-\infty}^{\infty} f(t)\,\theta(t)\,(\xi - t)\,dt. \tag{3.9}$$

Then, if we substitute the representation for θ given by (3.7) into (3.8) and (3.9) we obtain after evaluating the necessary integrals (numerically) two algebraic equations for K and θ_1, which when solved complete the solution.

The solutions $\theta(\xi)$ for values $a = 2{\cdot}0$, $1{\cdot}0$, $0{\cdot}5$, and $0{\cdot}1$ are shown in figure 2. In figure 3, θ_1 is plotted as a function of a. It is seen from figure 2 that as a decreases the thermal shock broadens. This could also have been inferred from the asymptotic solution for $\xi \to -\infty$ given by (3.5), the leading term of which is $1 + Ke^{a\xi}$. Also, it is seen from figure 3 that as $a \to 0$, $\theta_1 \to 13{\cdot}2$. We shall discuss this point in some detail, since we shall exploit the consequences of this behaviour in the analysis which follows.

The limiting behaviour for θ_1 as $a \to 0$ may be obtained as follows. We take $\theta(\xi)$ outside the integral in (3.8) by use of the mean-value theorem,

$$\theta_1 = 1 + \tfrac{2}{3}\theta(\xi_m) \int_{-\infty}^{\infty} f(t)\, dt, \tag{3.10}$$

where ξ_m is some point on the interval $-\infty < t < +\infty$. Since $f(t) = d(\ln \nu)/dt$, and $(\nu_1/\nu_0) = 4$, we may write

$$\theta_1 = 1 + \tfrac{2}{3}\theta(\xi_m) \ln 4.$$

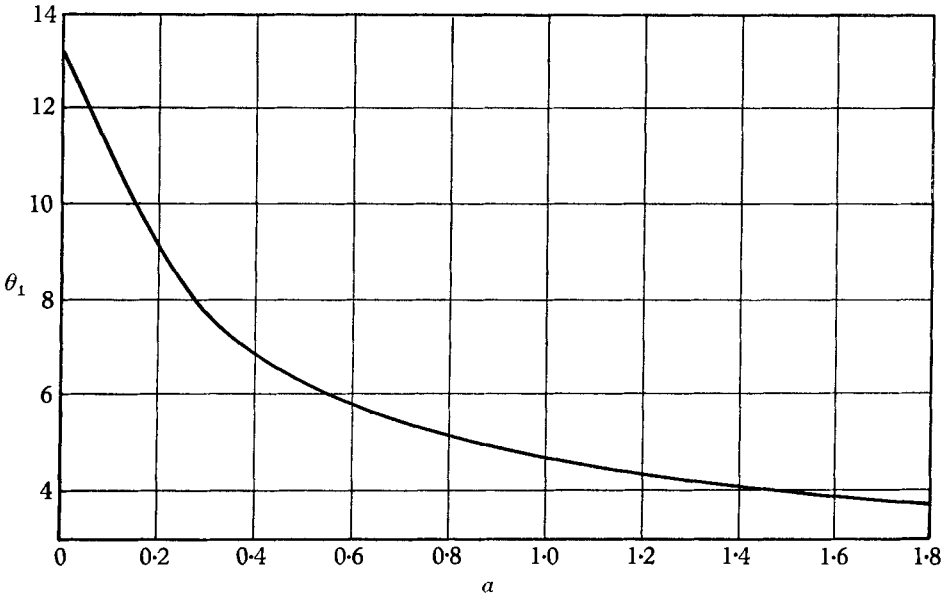

FIGURE 3. Maximum electron temperature θ_1 behind shock wave, as a function of parameter a, for the constant-conductivity, no-relaxation model.

Now, from figure 2 we observe that with decreasing values of the parameter a the temperature profiles $\theta(\xi)$ become broader and flatter. As $a \to 0$, θ tends to a substantially constant value (its downstream limit) over the range of ξ for which the function $f(\xi)$ is non-negligible. Therefore, we may choose ξ_m such that $\theta(\xi_m) = \theta_1$, and we obtain

$$\theta_1 = 1/(1 - \tfrac{3}{2}\ln 4) = 13{\cdot}158, \tag{3.11}$$

in agreement with the extrapolation of the curve shown in figure 3.

This last result suggests that the forcing function $f(\xi)$ may be replaced by a delta function when considering its influence on those quantities which are substantially constant over the non-vanishing domain of $f(\xi)$ and which are bounded over the entire domain $-\infty \leqslant \xi \leqslant +\infty$. Consistent with this, the density ratio ν and ion temperature ϕ should be replaced by step or Heaviside functions. This approach will be used in the analysis of the full equation (2.8). Before we proceed to the analysis of the full equation, a few remarks may be made about the direct effect of thermal conductivity on the thermal behaviour of the electrons during

their passage through the shock. For zero thermal conductivity (i.e. $a \to \infty$), equation (3.1) reduces to

$$d\theta/d\xi = \tfrac{2}{3} f(\xi)\,\theta$$

which, since $f(\xi) = dv/v\,d\xi$, can be integrated to obtain $\theta v^{-\frac{2}{3}} = \text{const.}$, and in particular

$$\theta_1/\theta_0 = (v_1/v_0)^{\frac{2}{3}} = 4^{\frac{2}{3}} \quad \text{for} \quad M \to \infty.$$

Thus, for zero thermal conductivity, we get the expected result that the compression of the electrons through the shock is isentropic. Now when the thermal conductivity become finite, part of the energy supplied to the electrons (from the ion-atom mixture) during the compression is carried away by conduction toward the region of lower electron temperature ahead of the shock. This process tends to lower the final electron temperature, but at the same time the electrons entering the compression zone have a higher temperature due to this preheating, and this tends to increase the final electron temperature. The net effect of these two competing mechanisms, as can be seen from the results obtained, is to *increase* the final temperature. Also, as the thermal conductivity becomes very large ($a \to 0$) the electron compression approaches an isothermal one, with all of the energy supplied to the electrons during this compression being transported ahead of the shock by conduction. Since essentially all of the thermal energy supplied to the electrons comes from the ion-atom mixture (recall that the kinetic energy of the electrons is negligible), what is implied by the foregoing is that as the thermal conductivity increases, so does this energy transfer. In an exact analysis, this increase in energy transfer would be reflected in a decrease in the final ion-atom temperature, but we neglect this perturbation, since we assume the gas to be slightly ionized with only a small fraction of the total internal energy content of the gas residing in the electrons.

Although the problem considered in this section is not physically realistic, since energy transfer between the electrons and the massive particles was neglected and as a consequence the downstream electron temperature was unrelated to the downstream ion-atom temperature, we shall see that the main qualitative features of the broadened electron temperature zone are unchanged when this energy transfer is taken into account.

4. Temperature-dependent thermal conductivity, with relaxation

Guided by the results of the previous section, we shall treat the solution of (2.8) with the following approximations.

(i) We replace $\nu(\xi)$ and $\phi(\xi)$ by Heaviside functions (Friedman 1957)

$$\nu = 1 + 3H(\xi), \quad \phi(\xi) = 1 + H(\xi)\,(\phi_1 - 1), \tag{4.1}$$

where

$$H(\xi) = 0 \quad \text{for} \quad \xi < 0$$
$$= 1 \quad \text{for} \quad \xi > 0.$$

(ii) From (i), it follows that we must replace $f(\xi)$ by a delta function,

$$f(\xi) = \delta(\xi) \ln 4. \tag{4.2}$$

The above approximations reduce (2.8) to

$$\frac{d}{d\xi}\left(\theta^{\frac{5}{2}}\frac{d\theta}{d\xi}\right) = a\frac{d\theta}{d\xi} - \tfrac{2}{3}a\ln 4\delta(\xi)\,\dot{\theta}(\xi) + (c/\theta^{\frac{3}{2}})\{1+3H(\xi)\}^2\{\theta-[1+H(\xi)(\phi_1-1)]\}. \tag{4.3}$$

The boundary conditions on (4.3) are

$$\theta = 1, \quad \frac{d\theta}{d\xi} = 0 \quad \text{at} \quad \xi = -\infty, \tag{4.4a}$$

$$\theta = \phi_1, \quad \frac{d\theta}{d\xi} = 0 \quad \text{at} \quad \xi = +\infty, \tag{4.4b}$$

where ϕ_1 is determined from (2.7*b*). We put $\eta = a\xi$, and express (4.3) as two differential equations,

$$\frac{d}{d\eta}\left(\theta^{\frac{5}{2}}\frac{d\theta}{d\eta}\right) = \frac{d\theta}{d\eta} + \frac{(c/a^2)}{\theta^{\frac{3}{2}}}(\theta-1) \quad \text{for} \quad \eta < 0 \tag{4.5a}$$

and

$$\frac{d}{d\eta}\left(\theta^{\frac{5}{2}}\frac{d\theta}{d\eta}\right) = \frac{d\theta}{d\eta} + \frac{16(c/a^2)}{\theta^{\frac{3}{2}}}(\theta-\phi_1) \quad \text{for} \quad \eta > 0, \tag{4.5b}$$

with the 'initial' conditions (4.4*a*) and (4.4*b*) applying respectively. The role of the delta function $\delta(\xi)$ in matching the solutions of (4.5*a*) and (4.5*b*) will become evident shortly. We observe that in (4.5) only the parameters ϕ_1 and c/a^2 appear. Since ϕ_1 is a function of M only, and it is shown in the Appendix that $c/a^2 = 6{\cdot}1(T_{e_0}/T_{m_0})/M^2 = 6{\cdot}1\tau/M^2$, the family of solutions obtained for a given Mach number and chosen values of τ will be applicable, within the limitations of the theory, for any slightly ionized gas. The specific gas properties enter only in the scale factor relating η to x.

If we linearize (4.5*a*) about $\xi = -\infty$ to obtain starting values for numerical integration we obtain

$$\frac{d^2(\theta-1)}{d\eta^2} = \frac{d(\theta-1)}{d\eta} + \frac{c}{a^2}(\theta-1). \tag{4.6}$$

The asymptotic solution to (4.5*a*) satisfying the boundary conditions (4.4*a*) is therefore

$$\theta - 1 = Ke^{\gamma_0\eta} \quad (\eta \to -\infty), \tag{4.7}$$

where

$$\gamma_0 = \tfrac{1}{2}\{1+(1+4c/a^2)^{\frac{1}{2}}\} \tag{4.8}$$

and K is as before an unknown parameter to be determined from the downstream boundary conditions. Similarly, we may linearise (4.5*b*) by replacing the terms $\theta^{\frac{5}{2}}$ and $\theta^{\frac{3}{2}}$ by $\theta_+^{\frac{5}{2}}$ and $\theta_+^{\frac{3}{2}}$ respectively, where θ_+ denotes the value of θ at $\xi = 0_+$. We obtain the differential equation

$$\frac{d^2\theta}{d\eta^2} = \frac{1}{\theta_+^{\frac{5}{2}}}\frac{d\theta}{d\eta} + \frac{16c}{a^2\theta_+^4}(\theta-\phi_1). \tag{4.9}$$

The solution of (4.9) which satisfies the boundary conditions (4.4*b*), and gives $\theta = \theta_+$ at $\xi = 0_+$ is

$$\theta = \theta_1 - (\theta_1-\theta_+)e^{-\gamma_1\eta} \quad (0_+ \leqslant \eta \leqslant \infty), \tag{4.10}$$

where

$$\gamma_1 = \frac{1}{2(\theta_+)^{\frac{5}{2}}}\left\{\left(1+\frac{64c}{a^2}\theta_+\right)^{\frac{1}{2}} - 1\right\}. \tag{4.11}$$

The use of the temperature θ_1 instead of θ_+ for evaluation of the transport coefficients would make only a small change in γ_1, provided θ_+/θ_1 is close to unity (as we expect it is, since according to the results of § 3 the major change in θ occurs *before* the ion compression represented by the Heaviside function at the origin). We observe also that as c tends to zero, γ_1 and $(d\theta/d\eta)_{\eta=0_+}$ both tend to zero; this is consistent with our requirement in § 3 that the solutions for zero relaxation satisfy the downstream boundary condition $(d\theta/d\xi)_{\xi=+\infty} = 0$.

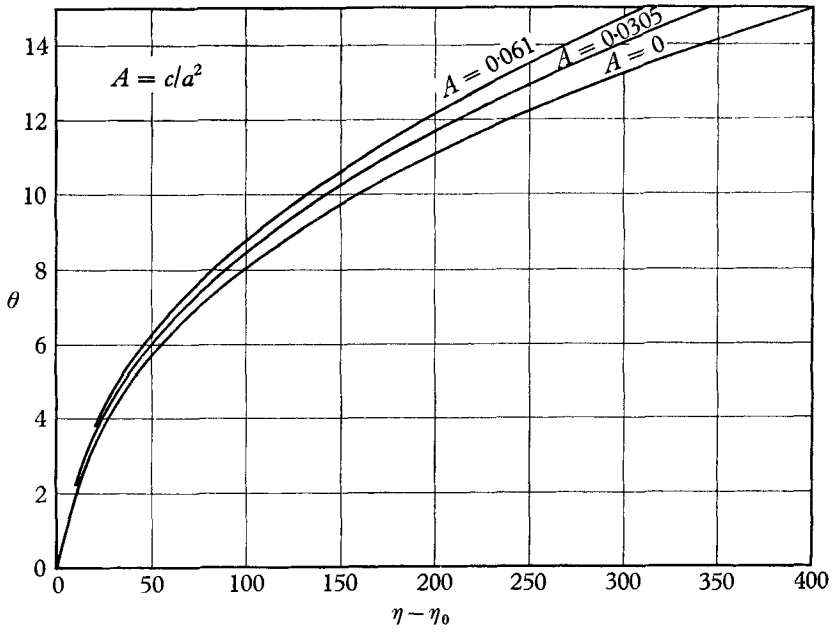

FIGURE 4. Non-dimensional electron temperature integrals of equation (4.5a) obtained for different values of the ratio c/a^2.

To complete the solution of (4.3) we require that the integral of (4.5a), started by the asymptotic expansion (4.7) and continued by numerical integration, match at $\eta = 0_+$ (where $\theta = \theta_+$) with the integral (4.10) of (4.5b). As in § 3, we have two unknown parameters, θ_+ and K, which must be determined in order to effect this matching. A procedure for accomplishing this without iteration is as follows.

For the numerical integration of (4.5a) we choose a convenient value of θ close to unity, say $\theta(\eta_0) = 1{\cdot}05$, corresponding to an as yet unknown $\eta = \eta_0$ near $-\infty$. From (4.7) we see that if $\theta(\eta_0)$ is specified, the starting conditions for the numerical integration will *not* involve the unknown quantity K (or its equivalent, η_0), since

$$(d\theta/d\eta)_{\eta=\eta_0} = \gamma_0[\theta(\eta_0) - 1], \quad (d^2\theta/d\eta^2)_{\eta=\eta_0} = \gamma_0^2[\theta(\eta_0) - 1].$$

Thus, for given values of a and c, and a chosen $\theta(\eta_0)$ which may be as close to unity as one desires, the integral of (4.5a) will be of the form $\theta - \theta(\eta_0) = f(\eta - \eta_0)$. Several such integral curves obtained for different values of $A = c/a^2$, starting with $\theta(\eta_0) = 1{\cdot}05$, are shown in figure 4.

To determine θ_+, we integrate (4.3) from $\eta = -\infty$ to $\eta = 0_+$, obtaining

$$\theta_+^{\frac{5}{2}}\left(\frac{d\theta}{d\eta}\right)_{0_+} = (\theta_+ - 1) - \tfrac{2}{3}\theta_+ \ln 4 + \frac{c}{a^2}\int_{-\infty}^{0_+} \frac{\theta - 1}{\theta^{\frac{3}{2}}}\, d\eta. \tag{4.12}$$

The term $-\frac{2}{3}\theta_+ \ln 4$ comes from the integration of the delta function past the origin to $\eta = 0_+$. Now, the integral on the right-hand side of (4.12) is, as was shown, a function only of known parameters and the value of θ at the upper limit, namely θ_+. Likewise, the derivative $(d\theta/d\eta)_{0_+}$ is a function only of known parameters and θ_+, from (4.10) and (4.11). Combining these equations we obtain an equation for θ_+ in the form

$$(\theta_1 - \theta_+)\left\{\left(16\frac{c}{a^2}\theta_+ + \tfrac{1}{4}\right)^{\frac{1}{2}} - \tfrac{1}{2}\right\} + 1 - (1 - \tfrac{2}{3}\ln 4)\,\theta_+ = \frac{c}{a^2}\int_{-\infty}^{0_+} \frac{\theta - 1}{\theta^{\frac{3}{2}}}\, d\eta, \tag{4.13}$$

which may be solved directly for θ_+. After θ_+ is found, the value of η_0 can then be determined, since $\theta = \theta_+$ at $\eta = 0$, and the integration of (4.5a) yielded $\theta - \theta(\eta_0)$ as a function of $\eta - \eta_0$. The complete solution is then composed of the asymptotic solution (4.7) and its numerical continuation from $\eta = -\infty$ up to $\eta = 0_+$, and the solution (4.10) from $\eta = 0_+$ to $\eta = +\infty$. It will be observed that the use of the delta function approximation for $f(\eta)$ forces a discontinuity in the derivative $(d\theta/d\eta)$ at the origin, such that

$$(d\theta/d\eta)_{0_-} - (d\theta/d\eta)_{0_+} = \tfrac{2}{3}\theta_+^{-\frac{3}{2}} \ln 4.$$

We have attempted to evaluate the accuracy of the foregoing method of solution by comparing its prediction of the electron temperature profile with that obtained by Jukes for a fully ionized gas at a Mach number of 10. The comparison is accomplished by replacing the Jukes ion density profile by a Heaviside function, and choosing $\tau = 1$, $c/a^2 = 6{\cdot}1/M^2$. The Mach number M which corresponds (for equality of the upstream velocity) to Jukes's value of 10 is $10\sqrt{2}$, because his case is that of a fully ionized gas in which the electrons contribute equally with the massive particles to the sound speed. We chose the downstream temperature ϕ_1 equal to that given by the Rankine–Hugoniot relations for $M = 10$, however, so as to have the same temperature ratio across the shock. The transport properties are evaluated for a proton-electron gas.

The comparison between the Jukes electron temperature profile and that given by the present theory is shown in figure 5. In both figure 5(a) and (b) the ion temperature profile ϕ is that found by Jukes and the abscissa is

$$\xi' = (3n_{i_0} m_i c_0 x)/4\mu_{i_0},$$

where the sound speed c is given by $c \doteq [5(p_i + p_e)/3n_i m_i]^{\frac{1}{2}}$. Hence, except for a numerical factor of order unity, $\xi' \approx x/l_{i_0}$, where l_{i_0} is the ion viscosity-based mean free path ahead of the shock. One sees that the present analysis predicts a somewhat more rapid approach of the electron temperature to its downstream equilibrium value than was found by Jukes, although in both analyses most of the electron temperature increase occurs ahead of the ion shock. The extent of the zone of elevated electron temperature ahead of the ion shock is approximately

the same for both theories (about 5×10^3 upstream mean free paths), and this predicted property of the shock structure is possibly the most interesting one and the one which might best be tested by experiment. To the scale to which figure 5 (*b*) has been plotted, the discontinuity in $d\theta/d\xi'$ at $\xi' = 0$ is not apparent.

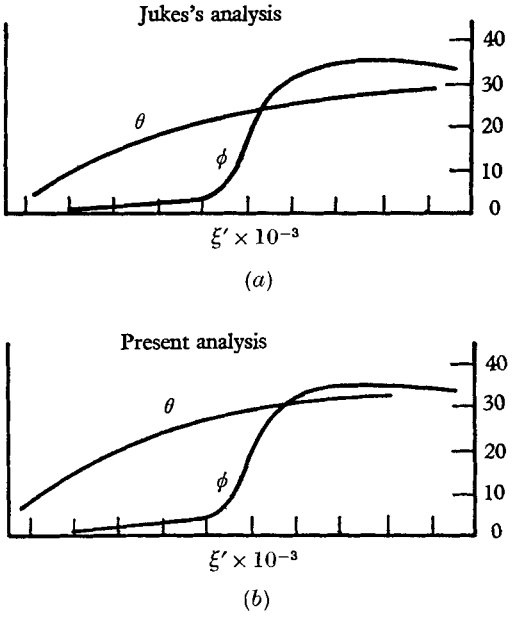

FIGURE 5. Comparison of the present analysis with Jukes's results for the electron temperature profile θ. In both (*a*) and (*b*), ϕ represents the non-dimensional ion temperature profile T_i/T_{i_0} obtained by Jukes, which in the present analysis was replaced by a Heaviside function. The non-dimensional length ξ' is the physical distance x normalized by the upstream mean free path.

5. The non-equilibrium shock wave

The analysis of the preceding section can be applied with little modification to the very interesting case where the temperature of the electrons differs from that of the ions and atoms in the free stream ahead of the shock. This situation is often met in practice, particularly in wind tunnels in which plasma produced by an electric arc is expanded rapidly in a nozzle to supersonic speeds (Sherman & Talbot 1961). It has been observed in such situations that the electron temperature in the supersonic stream is appreciably higher than the ion-atom temperature. This temperature differential appears to persist for a long time during the decay of the plasma, for reasons connected at least in part with the mechanism of recombination (Byron, Stabler & Bortz 1962).

The non-equality of the temperatures θ and ϕ ahead of the shock poses certain difficulties in prescribing the upstream boundary conditions for the shock. One way to treat the upstream boundary condition is as follows. When the oncoming gas is far upstream of the shock (supposing that $\theta > \phi$) one expects $d\theta/d\eta < 0$, since relaxation effects in the uniform stream will tend to make θ decrease and approach ϕ. As the gas nears the shock, this electron-temperature decrease will

be compensated for by an increase due to the thermal broadening effect produced by the shock wave. Somewhere ahead of the shock a place presumably is reached where the two effects compensate, and $d\theta/d\eta = 0$. We shall denote this point by η_0 and the non-dimensional electron and ion temperatures at this point, whatever they may be, by θ_0 and ϕ_0. We recall that the ion temperature T_i was non-dimensionalized by the upstream electron temperature T_{e_0}, so if $T_{i_0} < T_{e_0}$ the non-dimensional ion temperature at the point η_0 will be $\phi_0 = 1/\tau$, where $\tau = T_{e_0}/T_{i_0} \geqslant 1$. The existence of such a point η_0 is not guaranteed in all cases. For example, in a situation where the free-stream electron temperature is very much greater than the ion temperature the compressional heating of the electrons might not be great enough to counterbalance their cooling due to relaxation. The present analysis, without modification, would not be applicable in such a situation.

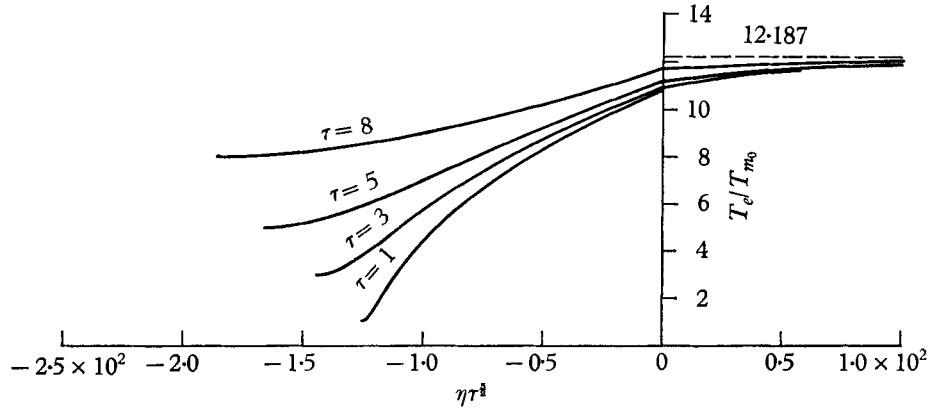

FIGURE 6. Mach 6 electron temperature profiles. The electron temperature is normalized with respect to the upstream massive-particle temperature T_{m_0}. The different curves represent different initial values of the upstream electron-massive particle temperature ratio $\tau = T_{e_0}/T_{m_0}$, and the physical length scale is normalized by $x = L\eta/a$ where L is the thickness of the massive-particle shock wave.

The solution for the non-equilibrium case is carried out in exactly the same way as was done for the equilibrium case, in § 4, with the following exceptions:

(i) In (4.3) the ion temperature 'profile' is replaced by

$$\phi = [1 + (\phi_1 - 1)\, H(\xi)]/\tau \tag{5.1a}$$

with

$$\tau = \theta(\eta_0)/\phi(\eta_0). \tag{5.1b}$$

Likewise, in the last terms on the right of (4.5*a*) and (4.5*b*) the factors in the parentheses are replaced by $(\theta - 1/\tau)$ and $(\theta - \phi_1/\tau)$ respectively. The quantity ϕ_1 is calculated just as before in terms of the ion-atom free-stream Mach number, through (2.7*b*).

(ii) Numerical integration of (4.5*a*) which is started from $\eta = \eta_0$, is begun with the boundary conditions $d\theta/d\eta = 0$, $\theta = 1$.

(iii) As in the previous section, once M and τ are chosen, the factors c/a^2 and ϕ_1 are specified, and no other transport property information is required to compute the integral curves of θ versus η.

Results of numerical integrations carried out on an IBM 7090 computer are shown in figures 6 to 9. For convenience, the electron temperature T_e has been normalized by the upstream ion-atom temperature T_{m_0}. The abscissa is $\eta\tau^{\frac{5}{2}}$, which was chosen because it groups the curves for different τ closely together. The spatial extent of the thermally broadened electron temperature zone can be related to $\eta\tau^{\frac{5}{2}}$ through (A 7) of the Appendix. If we denote by X and η_X the

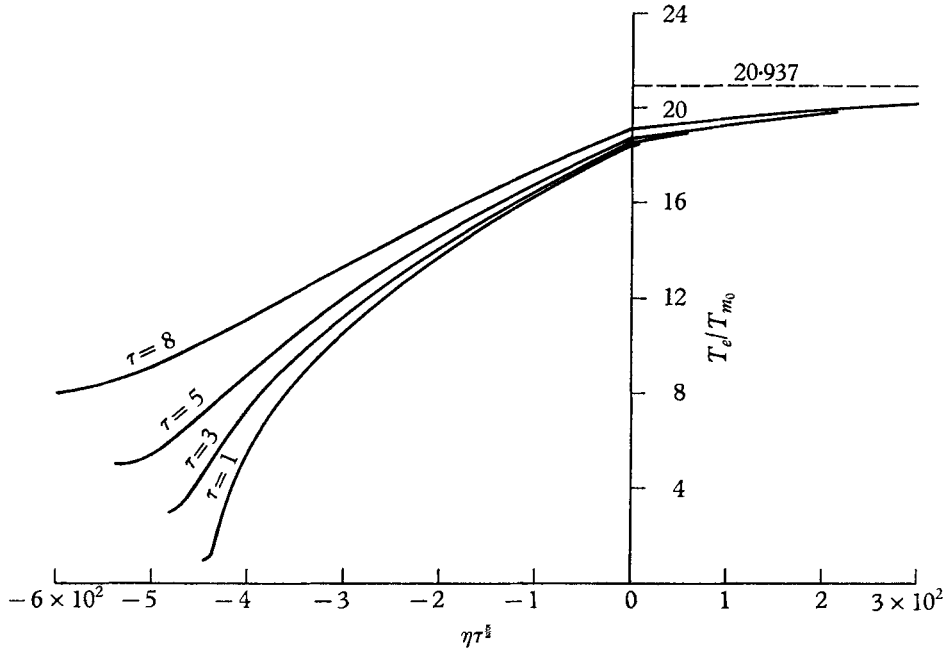

FIGURE 7. Mach 8 electron temperature profiles. The electron temperature is normalized with respect to the upstream massive-particle temperature T_{m_0}. The different curves represent different initial values of the upstream electron-massive particle temperature ratio $\tau = T_{e_0}/T_{m_0}$, and the physical length scale is normalized by $x = L\eta/a$ where L is the thickness of the massive-particle shock wave.

physical and transformed distances from the beginning of the electron temperature rise to the ion-atom shock ($x = 0$), we find from (A 7)

$$X = \frac{\tau^{\frac{5}{2}}\eta_X}{M}\left\{\frac{2{\cdot}2\times10^{11}T_{m_0}^2}{(\frac{5}{3}R_m)^{\frac{1}{2}}n_{e_0}\ln\Lambda_0}\right\},$$

where R_m is the specific gas constant for the massive particles. The quantity $\tau^{\frac{5}{2}}\eta_X/M$ has been plotted in figure 10. From figure 10 it is readily seen that X, the electron temperature zone, is for given values of the upstream conditions T_{m_0}, n_{e_0} and $\ln\Lambda_0$ appreciably increased with the Mach number, but only slightly increased with τ.

Before leaving this section, we shall comment briefly on the possible extension of this method to more highly ionized gases. We have assumed that the ionization is sufficiently small so that the energy content of the electrons is negligible compared to that of the massive particles (which are essentially all neutral atoms).

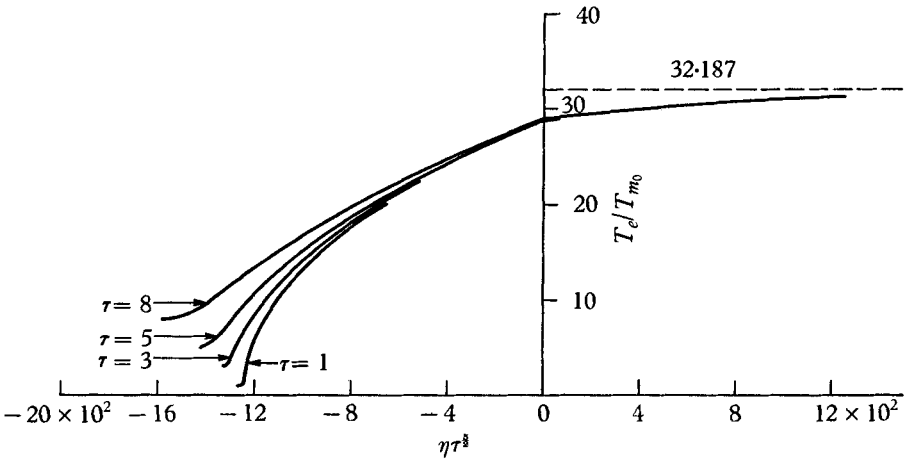

FIGURE 8. Mach 10 electron-temperature profiles. The electron temperature is normalized with respect to the upstream massive particle temperature T_{m_0}. The different curves represent different initial values of the upstream electron-massive particle temperature ratio $\tau = T_{e_0}/T_{m_0}$, and the physical length scale is normalized by $x = L\eta/a$ where L is the thickness of the massive particle shock wave.

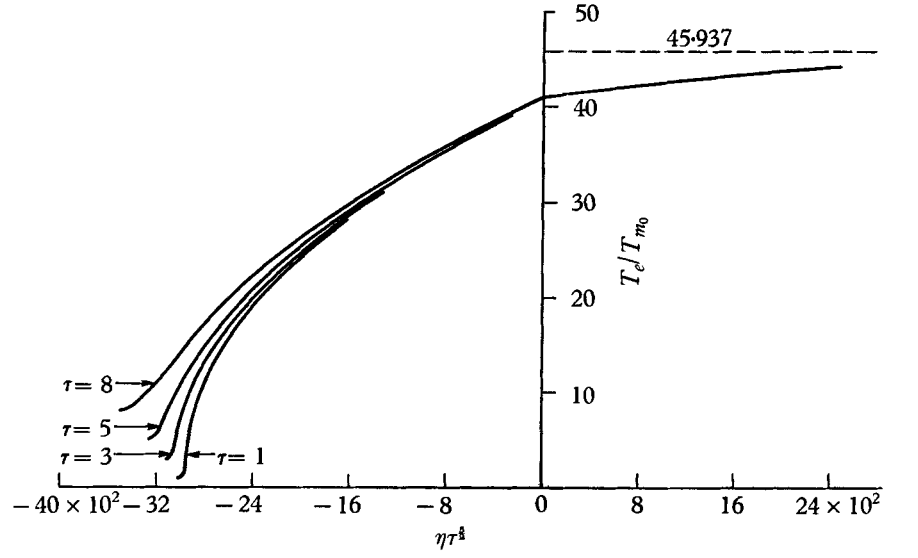

FIGURE 9. Mach 12 electron-temperature profiles.

This permitted us to specify in advance the downstream equilibrium temperature of the mixture, and to neglect the energy perturbation due to energy transfer between the electrons and massive particles. For larger ionization levels, this energy transfer could no longer be neglected and the corrected downstream equilibrium mixture temperature $(\bar{\phi}_1/\tau) = \bar{T}_{m_1}/T_{e_0}$ would instead be given by

$$\frac{\bar{\phi}_1}{\tau} = \frac{(\phi_1/\tau)}{(1+\bar{\alpha})} + \frac{\bar{\alpha}}{(1+\bar{\alpha})},$$

where ϕ_1/τ has the same meaning as before, and $\bar{\alpha} = n_i/(n_i + n_a)$ is the degree of ionization (n_a = number density of neutral atoms).

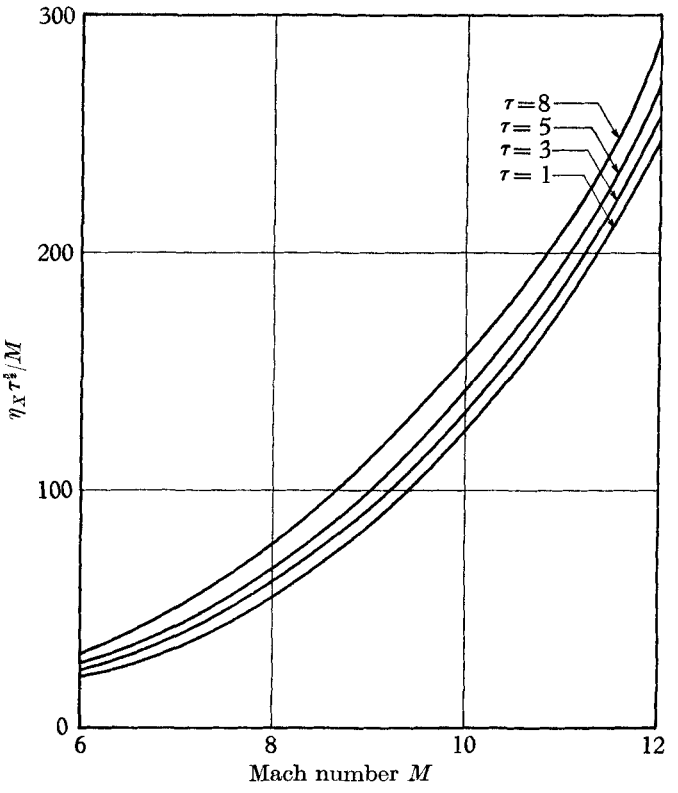

FIGURE 10. Non-dimensional width η_X of the zone of elevated electron temperature ahead of the massive-particle shock wave, as a function of Mach number and initial temperature ratio $\tau = T_{e_0}/T_{m_0}$.

6. Electric field and charge separation

It was mentioned in the introduction that a small charge separation is produced within the shock transition. We consider this effect now. The one-dimensional momentum equation for the electron gas is

$$\frac{d}{dx}(m_e n_e u_e^2) + \frac{d}{dx}(n_e k T_e) - \tfrac{4}{3}\mu_e \frac{du_e}{dx} + n_e e E - P^{em} = 0, \tag{6.1}$$

in which E is the electric field produced by the charge separation. Using the same arguments which were applied to the energy equation, we neglect the electron kinetic energy, viscous stress and momentum exchange terms, which then reduces (6.1) to

$$E = -\frac{k}{eL}\left\{\frac{T_e}{\nu_e}\frac{d\nu_e}{d\xi} + \frac{dT_e}{d\xi}\right\}. \tag{6.2}$$

Poisson's equation may be written

$$dE/d\xi = 4\pi n_{e_0} eL(\nu_i - \nu_e), \tag{6.3}$$

where $\nu_i = n_i/n_{e_0}$, $\nu_e = n_e/n_{e_0}$. After differentiating (6.2) and combining with (6.3), we obtain

$$(\nu_i - \nu_e) = -\frac{k}{4\pi n_{e_0} e^2 L^2}\frac{d}{d\xi}\left\{\frac{T_e}{\nu_e}\frac{d\nu_e}{d\xi} + \frac{dT_e}{d\xi}\right\}. \tag{6.4}$$

From order of magnitude arguments, we conclude that the derivative of the term in the braces will at most be of order T_{e_1}, and since $n_{e_1} \leqslant 4n_{e_0}$, a rough order of magnitude for the charge separation is

$$(\nu_e - \nu_i) \sim (l_{D_1}/L)^2,$$

where $l_{D_1} = (kT_{e_1}/4\pi n_{e_1} e^2)^{\frac{1}{2}}$ is the Debye length based on downstream conditions. Since for almost all conditions of interest $(l_D/L)^2 \ll 1$, we conclude that charge separation is very small, and may be neglected in computing the electron temperature profile. This conclusion was also reached by Jukes. This charge separation, however, is sufficient to produce an electric field which is important in the over-all energy balance. We may examine the consequence of this electric field by computing the work W done by the electric field on an electron in its passage through the shock transition.

From (6.2)

$$W = -\int_{-\infty}^{\infty} eE\,dx = k\int_{-\infty}^{\infty} \frac{T_e}{\nu_e} d\nu_e + k\int_{-\infty}^{\infty} dT_e. \tag{6.5}$$

Since most of the electron temperature rise occurs ahead of the density change, for a strong shock we have

$$W \approx kT_{e_1} \ln 4 + k(T_{e_1} - T_{e_0}). \tag{6.6}$$

The first term of (6.6) is the work done on an electron in an isothermal compression through the shock, at the temperature T_{e_1}. This is in agreement with what we have already observed, that the pre-heating of the electrons by thermal conduction makes their compressions almost isothermal and the work for this isothermal compression is supplied by the electric field. The second term of (6.6) is 2/5 the enthalpy increase per electron. This indicates that the electric field is responsible as well for part of the heating of the electrons, the remaining part being supplied by the collisional relaxation process.

7. Effects of ionization and recombination

Since ionization and recombination rates vary widely with the state and composition of the gas, it does not seem feasible to discuss these processes in any generality. Instead we shall attempt to illustrate their effects on the shock structure by examination of a particular case. Consider a shock wave in argon, with the following free-stream conditions: $n_{e_0} = 10^{14}\,\mathrm{cm}^{-3}$, $n_{m_0} = 10^{16}\,\mathrm{cm}^{-3}$, $u_0 = 5 \times 10^5\,\mathrm{cm\,sec}^{-1}$, $T_{e_0} = 3500°\,\mathrm{K}$, $T_{m_0} = 700\,°\mathrm{K}$, $M = 10$. These plasma conditions are similar to those obtained in the Berkeley arc-heated low-density wind tunnel. For these conditions the ionization rate is exceedingly small, and the dominant mechanism for change in electron density is recombination.

It has been shown (Hinnov & Hirschberg 1962; Byron *et al.* 1962) that under conditions such as those assumed here, the recombination process is the three body process

$$A^+ + e + e \rightarrow A^* + e. \tag{7.1}$$

The excited atom A^* thus formed is at first de-excited to lower energy levels by inelastic collisions with free electrons, and thereafter to the ground state by

radiative de-excitation. Hinnov & Hirschberg find from their analysis that the recombination coefficient $\dot{\alpha} = -(1/n_e^2)(dn_e/dt)$ can be expressed approximately by

$$\alpha \approx 5{\cdot}6 \times 10^{-27} (T_{\mathrm{eV}})^{-\frac{9}{2}} n_e \,\mathrm{cm^3\,sec^{-1}}, \tag{7.2}$$

where T_{eV} is the electron temperature in electron volts. The strong dependence of α on T_{eV} is worth noting. If we evaluate α at the upstream temperature $T_{\mathrm{eV}_0} = 0{\cdot}3\,\mathrm{eV}$ we obtain $\alpha \approx 1{\cdot}3 \times 10^{-10}\,\mathrm{cm^3\,sec^{-1}}$. On the other hand, if we use the electron temperature just ahead of the ion shock, $T_{\mathrm{eV}_1} \approx 1{\cdot}7\,\mathrm{eV}$, we obtain according to (7.2) $\alpha \approx 4{\cdot}8 \times 10^{-14}$, although the recombination theory is not accurate for such high electron temperatures.

To interpret the value of α we require the approximate extent of the electron temperature shock wave. From (A 7) we find $X/\eta = 0{\cdot}52$, and hence from figure 9, $X \approx 13\,\mathrm{cm}$. The broadness of the electron temperature zone is evident from these values. If we take for rough estimation the mean value $\bar{\alpha} \approx 10^{-12}$ $\mathrm{cm^{-3}\,sec^{-1}}$, we find, using $dn_e/dt = u_0(dn_e/dx)$ in the definition of α,

$$n_e/n_{e_0} = u_0/(u_0 + \bar{\alpha} n_{e_0} X), \tag{7.3}$$

which for $X = 13\,\mathrm{cm}$ and the assumed upstream conditions gives about $0{\cdot}26\,\%$ decrease in the ionization. (If we had used the upstream electron temperature, the decrease would have come out over $25\,\%$.) These simple estimates indicate that under some circumstances the recombination could be appreciable, and would have to be taken into account in the calculations.

Another quantity of interest in connexion with the recombination process is the energy fed back into the electron gas by the inelastic electron-atom collisions. The energy gained by the free electrons per recombination is not too accurately known, because of uncertainties involved in the de-excitation of metastable states (Byron *et al.*), but for argon this energy transfer is about $0{\cdot}8\,\mathrm{eV}$ per recombination. Thus, if recombination caused a $2{\cdot}6 \times 10^{11}$ decrease in electron number density within the electron shock zone, a total energy transfer of about $2{\cdot}1 \times 10^{11}$ eV per $\mathrm{cm^3}$ to the electron gas would be associated with this recombination. This value is to be compared with the total energy content of $3 \times 10^{13}\,\mathrm{eV\,per\,cm^3}$. Clearly, when recombination cannot be neglected, neither can the energy transfer due to inelastic collisions. It is in fact this energy transfer which is mainly responsible for the persistance of high electron temperatures in certain recombining plasmas.

For comparison, we may examine the values of the ion-atom shock thickness. According to the Mott-Smith theory (figure 11), for neutral argon the shock thickness L is about six times the upstream mean free path l_{m_0}. On the other hand, if the ionization were sufficiently high, such that the inter-molecular collisions were dominated by coulombic interaction ($s = 2$), we see that L would be several hundred times as large as l_{m_0}. The viscosity of argon at 700 °K is $4{\cdot}4 \times 10^{-4}$ g/cm sec, and the viscosity-based mean free path for this temperature and $n_m = 10^{16}\,\mathrm{cm^{-3}}$ is $l_{m_0} = 2{\cdot}7 \times 10^{-2}\,\mathrm{cm}$, so the neutral atom shock thickness for the assumed conditions would be of the order of $0{\cdot}13\,\mathrm{cm}$. Thus the thermally broadened electron temperature shock is according to these estimates some 10^2 upstream mean free paths in extent.

To complete the discussion of recombination phenomena, we observe from (7.2) that according to our solution of the shock structure problem the region of elevated electron temperature ahead of the compression zone will be a region of reduced recombination rate, since in this region $n_e = n_{e_0}$ while T_e increases. We believe that this reduction in recombination rate provides the explanation for the 'dark space' which we have observed ahead of shock waves in the partially ionized flows produced in the Berkeley arc-heated low-density wind tunnel (Sherman & Talbot 1961), since the self-luminosity of the flow in this case is due to the recombination radiation. Typical observations of such shock waves and associated dark spaces are shown in figure 12, plate 1. Detailed studies of such shock waves are in progress, and will be reported on in a future publication.

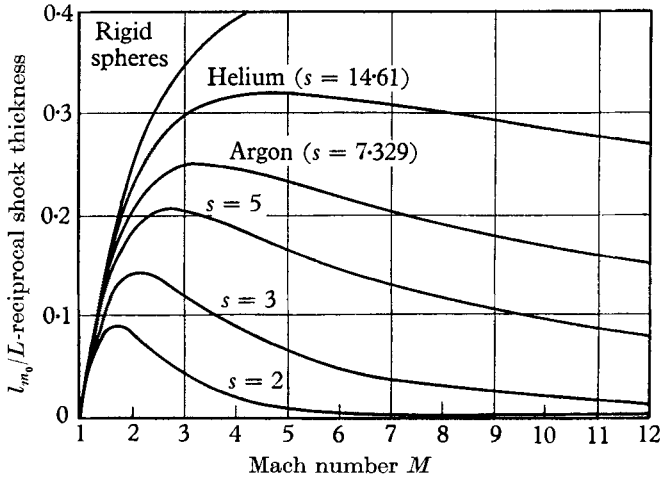

FIGURE 11. Maximum-slope shock thicknesses from Mott-Smith theory for repulsive point-centre molecules, normalized by the upstream mean free path l_{m_0} (after Muckenfuss).

8. Concluding remarks

The model of the shock structure which we have proposed offers a relatively simple method for analysing shock waves under both equilibrium and non-equilibrium conditions in a slightly ionized gas. The predictions obtained from this model are qualitatively similar to those found by Jukes for a fully ionized gas, the essential feature of the shock transition being the broad region of elevated electron tempertaure which extends ahead of the compression zone of the shock wave.

A difficulty in applying the present analysis to physical situations is the lack of information on the transport properties (viscosity, thermal conductivity, energy exchange) in a non-equilibrium partially ionized gas. For simplicity, and to illustrate the method of analysis, we used the thermal-conductivity and energy-exchange expressions appropriate to a fully ionized gas, although we recognize that these may not be realistic values for slightly ionized gases. In particular, we expect the electron thermal conductivity in a slightly ionized gas to be numerically smaller and to vary differently with temperature than the five-halves power law appropriate to a fully ionized gas. Consequently, we expect

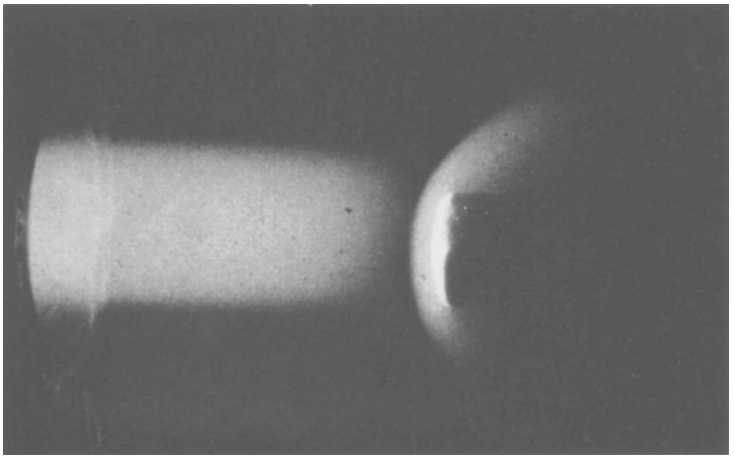

(*a*)

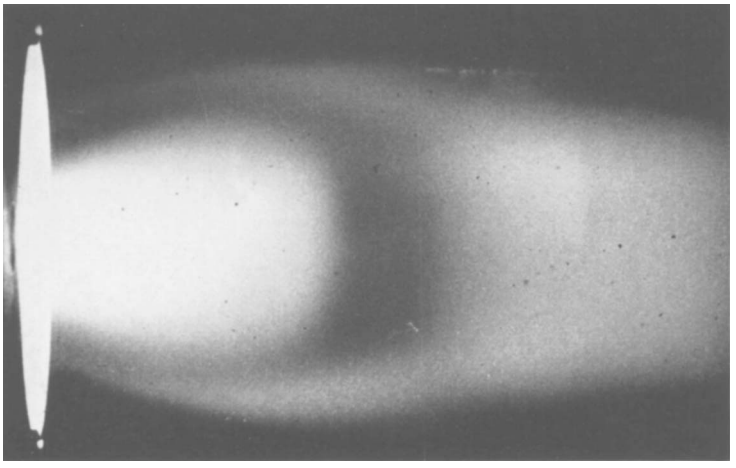

(*b*)

FIGURE 12, plate 1. (*a*) Shock wave formed ahead of $\frac{5}{8}$ in. diameter flat-ended cylinder in $M = 6{\cdot}2$ free jet argon flow issuing from a conical nozzle. Ionization $\sim 0{\cdot}6\,\%$, stagnation pressure and temperature ~ 300 mm Hg and 5000 °K, test chamber pressure $\sim 300\,\mu$ Hg.

(*b*) Free expansion of argon from $\frac{1}{2}$ in. diameter sonic nozzle. Stagnation pressure and temperature ~ 250 mm Hg and 7000 °K, test chamber pressure $\sim 700\,\mu$ Hg. Ionization $\sim 1\,\%$. Distance from exit of nozzle to beginning of dark space ahead of normal shock is approximately 4 in., and the dark space extends for about 1·1 in. The Mach number ahead of the normal shock (at rear of dark space) is in the vicinity of 10. Notice also the dark spaces associated with the 'barrel shocks' surrounding the jet.

that for a partially ionized gas the zone of elevated electron temperature may be considerably smaller in extent than that predicted here. Fortunately, it is a simple matter in our analysis to utilize any desired expressions for the electron transport properties and electron-atom energy exchange.

The research reported here was supported by the Air Force Office of Scientific Research under Contract AF 49(638)–502.

Appendix

We present here some useful formulas for the constants a, b, c, and for converting the lengths η and ξ to the physical distance x.

The quantity a was defined as

$$a = \tfrac{3}{2}(n_{e_0} u_0 L/\lambda_{e_0}). \tag{A 1}$$

If we use the Spitzer–Härm (1953) value for the thermal conductivity,

$$\lambda_{e_0} = \frac{\frac{9}{2}(2/\pi)^{\frac{3}{2}}(kT_{e_0})^{\frac{5}{2}}}{m_e^{\frac{1}{2}} e^4 \ln \Lambda_0}, \quad \Lambda_0 = \frac{3}{2e^3}\left(\frac{k^3 T_{e_0}^3}{\pi n_{e_0}}\right)^{\frac{1}{2}}, \tag{A 2}$$

we obtain

$$a = \tfrac{1}{3}(\tfrac{1}{2}\pi)^{\frac{3}{2}} \frac{m_e^{\frac{1}{2}} e^4 n_{e_0} u_0 L \ln \Lambda_0}{(kT_{e_0})^{\frac{5}{2}}}$$

$$\doteq 4{\cdot}5 \times 10^{-12} \frac{L n_{e_0} u_0 \ln \Lambda_0}{T_{e_0}^{\frac{5}{2}}}. \tag{A 3}$$

Also, using the definitions of a and c, we obtain

$$\frac{c}{a^2} = \frac{96}{5\pi} \frac{(T_{e_0}/T_{m_0})}{M^2} \doteq 6{\cdot}1 \frac{\tau}{M^2}. \tag{A 4}$$

For an estimate of the constant b, we may use the Lorentz value for μ_e, namely (Kaufman 1960),

$$\mu_{e_0}/\lambda_{e_0} = \tfrac{32}{135} m_e. \tag{A 5}$$

Then

$$b = \frac{4}{3}\frac{\mu_{e_0}}{kT_{e_0}}\frac{u_0^2}{\lambda_{e_0}} = \frac{128}{405}\frac{u_0^2}{(kT_{e_0}/m_e)}. \tag{A 6}$$

Using typical values of b and a (cf. § 7), it is easily seen that $b/a < 10^{-2}$, thus justifying the neglect of the viscosity terms in the momentum and energy equations for the electrons.

The physical distance x, in terms of the non-dimensional length η, is given by

$$\frac{x}{\eta} = \frac{L}{a} \doteq \frac{2{\cdot}2 \times 10^{11} T_{e_0}^{\frac{5}{2}}}{n_{e_0} u_0 \ln \Lambda_0}. \tag{A 7}$$

It will be noticed that in this relationship the ion-atom shock thickness L cancels out. This was to be expected, since the ion-atom shock profile was replaced by a 'zero-thickness' Heaviside function. It is, however, of interest to compare the electron and ion-atom shock thicknesses. For this purpose, the results computed by Muckenfuss (1960) for molecules which are point centres of repul-

sion, reproduced in figure 11, are useful. The reference mean free path l_{m_0} used by him is the viscosity mean free path based on conditions ahead of the shock,

$$l_{m_0} = \frac{16\mu_{m_0}}{5n_{m_0}(2\pi m_m kT_{m_0})^{\frac{1}{2}}} \doteq \frac{1{\cdot}65\mu_{m_0}}{\rho_{m_0}a_{m_0}}, \tag{A 8}$$

where μ_{m_0}, ρ_{m_0} and a_{m_0} are respectively the free stream viscosity, density and sound speed in the ion-atom mixture. In figure 11, s is the exponent in the intermolecular force law, $F = \kappa/r^s$, and according to this model $\mu_m \sim (T_m)^{(s+3)/2(s-1)}$.

REFERENCES

Byron, S., Stabler, R. C. & Bortz, P. I. 1962 *Phys. Rev. Letters*, **8**, 376.

Friedman, B. 1957 *Principles and Techniques of Applied Mathematics*, Ch. 3. New York: J. Wiley and Sons.

Greenberg, O. W., Sen, H. K. & Treve, Y. M. 1960 *Phys. Fluids*, **3**, 379.

Hinnov, E. & Hirschberg, J. G. 1962 *Phys. Rev.* **125**, 795.

Jukes, J. O. 1957 *J. Fluid Mech.* **3**, 275.

Kaufman, A. N. 1960 *The Theory of Neutral and Ionized Gases* (ed. C. De Witt & J. F. Detouf). New York: J. Wiley and Sons.

Mott-Smith, H. M. 1951 *Phys. Rev.* **82**, 885.

Muckenfuss, C. 1960 *Phys. Fluids*, **3**, 320.

Post, R. 1956 *Rev. Mod. Phys.* **28**, 338.

Sherman, F. S. & Talbot, L. 1961 *Hypersonic Flow Research* (ed. F. R. Riddell). New York: Academic Press.

Spitzer, L. 1956 *Physics of Fully Ionized Gases*, Ch. 5. New York: Interscience.

Spitzer, L. & Härm, R. 1953 *Phys. Rev.* **89**, 977.

Talbot, L. 1962 *J. Amer. Rocket Soc.* **32**, 1009.

Tidman, D. A. 1958 *Phys. Rev.* **111**, 1439.

Tricomi, F. 1957 *Integral Equations*, Ch. 1. New York: Interscience.